Clonally expanding smooth muscle cells promote atherosclerosis by escaping efferocytosis and activating the complement cascade

Ying Wang[a,b], Vivek Nanda[a,b,c], Daniel Direnzo[a], Jianqin Ye[a], Sophia Xiao[a], Yoko Kojima[a], Kathryn L. Howe[a], Kai-Uwe Jarr[a], Alyssa M. Flores[a], Pavlos Tsantilas[a], Noah Tsao[a], Abhiram Rao[b,d], Alexandra A. C. Newman[e], Anne V. Eberhard[a], James R. Priest[f], Arno Ruusalepp[g], Gerard Pasterkamp[h,i], Lars Maegdefessel[j,k], Clint L. Miller[l,m,n], Lars Lind[o], Simon Koplev[p], Johan L. M. Björkegren[p], Gary K. Owens[e], Erik Ingelsson[b,o,q], Irving L. Weissman[r,1], and Nicholas J. Leeper[a,b,1]

[a]Division of Vascular Surgery, Department of Surgery, Stanford University School of Medicine, Stanford, CA 94305; [b]Stanford Cardiovascular Institute, Stanford University, Stanford, CA 94305; [c]Department of Molecular and Cellular Pathology, University of Alabama at Birmingham, Birmingham, AL 35294; [d]Department of Bioengineering, Stanford University, Stanford, CA 94305; [e]Robert M. Berne Cardiovascular Research Center, University of Virginia, Charlottesville, VA 22904; [f]Division of Pediatric Cardiology, Department of Pediatrics, Stanford University School of Medicine, Stanford, CA 94305; [g]Department of Cardiac Surgery, Tartu University Hospital, Tartu, Estonia 50406; [h]Department of Cardiology, University Medical Center Utrecht, 3584CX Utrecht, the Netherlands; [i]Laboratory of Clinical Chemistry, University Medical Center Utrecht, 3584CX Utrecht, the Netherlands; [j]Department for Vascular and Endovascular Surgery, Klinikum Rechts der Isar, Technical University Munich, 80333 Munich, Germany; [k]German Center for Cardiovascular Research (DZHK partner site), 10785 Munich, Germany; [l]Center for Public Health Genomics, Department of Public Health Sciences, University of Virginia, Charlottesville, VA 22904; [m]Department of Biochemistry and Molecular Genetics, University of Virginia, Charlottesville, VA 22904; [n]Department of Biomedical Engineering, University of Virginia, Charlottesville, VA 22904; [o]Department of Medical Sciences, Uppsala University, SE-751 05 Uppsala, Sweden; [p]Department of Genetics and Genomic Sciences, Icahn Institute for Genomics and Multiscale Biology, Icahn School of Medicine at Mount Sinai, New York, NY 10029-6574; [q]Division of Cardiovascular Medicine, Department of Medicine, Stanford University School of Medicine, Stanford, CA 94305; and [r]Institute for Stem Cell Biology and Regenerative Medicine, Stanford University School of Medicine, Stanford, CA 94305

Contributed by Irving L. Weissman, April 20, 2020 (sent for review April 8, 2020; reviewed by Joshua Beckman and Yogen Kanthi)

Atherosclerosis is the process underlying heart attack and stroke. Despite decades of research, its pathogenesis remains unclear. Dogma suggests that atherosclerotic plaques expand primarily via the accumulation of cholesterol and inflammatory cells. However, recent evidence suggests that a substantial portion of the plaque may arise from a subset of "dedifferentiated" vascular smooth muscle cells (SMCs) which proliferate in a clonal fashion. Herein we use multicolor lineage-tracing models to confirm that the mature SMC can give rise to a hyperproliferative cell which appears to promote inflammation via elaboration of complement-dependent anaphylatoxins. Despite being extensively opsonized with pro-phagocytic complement fragments, we find that this cell also escapes immune surveillance by neighboring macrophages, thereby exacerbating its relative survival advantage. Mechanistic studies indicate this phenomenon results from a generalized opsonin-sensing defect acquired by macrophages during polarization. This defect coincides with the noncanonical up-regulation of so-called don't eat me molecules on inflamed phagocytes, which reduces their capacity for programmed cell removal (PrCR). Knockdown or knockout of the key antiphagocytic molecule CD47 restores the ability of macrophages to sense and clear opsonized targets in vitro, allowing for potent and targeted suppression of clonal SMC expansion in the plaque in vivo. Because integrated clinical and genomic analyses indicate that similar pathways are active in humans with cardiovascular disease, these studies suggest that the clonally expanding SMC may represent a translational target for treating atherosclerosis.

atherosclerosis | clonality | smooth muscle cells | efferocytosis | CD47

Despite being the world's leading killer (1), the root causes of atherosclerotic cardiovascular disease remain elusive (2, 3). This is due in part to the fact that cells which contribute to growing atherosclerotic plaque frequently undergo extensive phenotypic modulation, wherein they down-regulate the very "cell-specific" markers needed for their definitive identification (4). This process is commonly referred to as "dedifferentiation" in the field of vascular biology. As a result, there are major ambiguities regarding the origins of the individual components of the plaque and how they contribute to disease pathogenesis. This is one of the reasons why all currently approved therapies target risk factors for disease (e.g., hypertension, diabetes, and hyperlipidemia) rather than the cells that actually constitute the lesion.

While there is little doubt that bone marrow-derived inflammatory cells home to the developing lesion (3, 5), emerging

Significance

Cardiovascular disease remains the world's leading killer, despite the widespread use of cholesterol-lowering medicines. Recent studies suggest a portion of this residual risk may result from the clonal expansion of cells within the atherosclerotic plaques of diseased blood vessels. How these cells promote inflammation and whether they can be therapeutically targeted remain unclear. The current study suggests that clonally expanding cells may cause disease by triggering the complement cascade while evading immune surveillance. However, these cells also appear to be susceptible to therapies that reactivate phagocytic clearance pathways, suggesting a potential treatment approach for heart disease similar to current oncology efforts directed against the cancer stem cell.

Author contributions: Y.W., D.D., Y.K., J.R.P., L.M., G.K.O., E.I., and N.J.L. designed research; I.L.W. guided experimental design; Y.W., V.N., D.D., J.Y., S.X., Y.K., K.L.H., K.-U.J., A.M.F., P.T., N.T., A. Rao, A.A.C.N., A.V.E., J.R.P., G.P., L.M., J.L.M.B., E.I., and N.J.L. performed research; Y.W., A.A.C.N., J.R.P., A. Ruusalepp, G.P., L.M., C.L.M., L.L., S.K., J.L.M.B., G.K.O., E.I., I.L.W., and N.J.L. contributed new reagents/analytic tools; Y.W., V.N., D.D., J.Y., Y.K., K.L.H., K.-U.J., A.M.F., J.R.P., G.P., L.M., C.L.M., L.L., S.K., J.L.M.B., G.K.O., E.I., and N.J.L. analyzed data; I.L.W. provided feedback on data; and Y.W., K.-U.J., G.K.O., E.I., and N.J.L. wrote the paper.

Reviewers: J.B., Vanderbilt University Medical Center; and Y.K., University of Michigan.

Competing interest statement: I.L.W. and N.J.L. are cofounders of Forty Seven, Inc., an immunooncology company. This company was recently acquired by Gilead Sciences; the purchase did not include stock in Gilead. I.L.W. and N.J.L. do not currently have any consulting agreement with Gilead Sciences.

Published under the PNAS license.

[1]To whom correspondence may be addressed. Email: irv@stanford.edu or nleeper@stanford.edu.

This article contains supporting information online at https://www.pnas.org/lookup/suppl/doi:10.1073/pnas.2006348117/-/DCSupplemental.

First published June 15, 2020.

Downloaded at Palestinian Territory, occupied on December 4, 2021

www.manaraa.com

data suggest that it is a phenotypically-modulated ("dedifferentiated") cell in the vascular smooth muscle cell (SMC) lineage which may actually give rise to the majority of cells within the atherosclerotic plaque (6, 7). Sophisticated lineage-tracing studies revealed that the progeny of these cells have remarkable plasticity and can assume a wide variety of phenotypes. These range from cells which resemble cap-stabilizing myofibroblasts (which are likely beneficial), to cells previously assumed to represent bone marrow-derived macrophages (which are likely detrimental), and even to cells which express stem cell markers (whose role is unknown) (6, 8–13). This final point is important because Benditt and colleagues reported a clonal origin of human atherosclerosis nearly 50 y ago (14), and recent studies revealed that murine SMCs can expand in a clonal fashion under periods of stress (7, 8, 10).

These data indicate that there may be a cell which resembles an "atherosclerotic stem cell," akin to cancer stem cells or their clonal precursors (15). They also raise the interesting possibility that it might be translationally targetable, similar to ongoing efforts in the field of oncology (16). However, the biology of the clonally expanding SMC remains incompletely defined, and no therapies yet exist which can specifically suppress this particular cell type in vivo. In this report, we set out to define the molecular mechanisms by which this cell promotes vascular inflammation. We aimed to identify the source of its relative survival advantage and determine how it escapes immune surveillance. Results from these murine lineage-tracing studies were then intersected with data derived from biobanked human samples, so as to establish their relevance to clinical cardiovascular disease. Finally, a therapeutic intervention study was performed to determine whether the clonal SMC can be precision-targeted, and if this approach could lessen plaque burden without disrupting those SMCs which give rise to and stabilize the fibrous cap.

Results

Clonally Expanding SMCs Up-Regulate Complement C3 during Atherogenesis. Using a multicolor SMC lineage tracer ("Rainbow" mouse), we first confirmed prior reports (11) that early during atherogenesis a subset of SMCs dedifferentiate and up-regulate the classic stem cell marker Sca1 (*SI Appendix*, Fig. S1 *A* and *B*). With continued exposure to a high-fat "Western" diet, these cells progressively expanded and coalesced into clonal patches of SMCs (Fig. 1 *A* and *B* and *SI Appendix*, Fig. S1 *C–E*). We observed Sca1 staining to be most intense within the core of the dominant clone, and found that the size of the dominant clone directly correlated with total lesion size (*SI Appendix*, Fig. S1*F*). These Sca1-expressing cells appeared to be distinct from the previously described "transdifferentiated" macrophage-like cells (6), and tended to colocalize near the necrotic core of the plaque (Fig. 1*C* and *SI Appendix*, Fig. S1*G*).

Using Sca1 as a marker gene, we next set out to define the biology of the clonally expanding SMC. Single-cell RNA-seq (sequencing) of SMC-derived cells from the plaques of a single-color SMC lineage tracer ("Tomato" mouse) revealed that the Sca1$^+$ subpopulation has a distinct gene expression profile compared with other clusters of SMC-derived cells (*SI Appendix*, Fig. S2). Pathway analyses indicated that these SMCs are highly dedifferentiated, evidenced by their down-regulation of classic SMC markers and up-regulation of factors related to innate immunity, inflammation, and the classical complement cascade (Fig. 1*D*). Within the cluster of Sca1$^+$ SMCs, C3 was a defining hub gene (module correlation $P = 1.08 \times 10^{-41}$) and one of the most significantly up-regulated factors (4.37-fold increase; Fig. 1*E*).

Patients with Cardiovascular Disease Have High Levels of Circulating C3 and Human Atherosclerotic Plaques Express Genes Found on the Murine Clonally Expanding SMC. In an effort to establish the translational relevance of these findings, we next performed a series of analyses with human samples. Specifically, we tested 1) whether systemic C3 expression is associated with risk for coronary artery disease (CAD); 2) if the dedifferentiated SMC is a source of C3 in human plaque; and 3) if CAD patients harbor a C3-producing cell that resembles the Sca1$^+$ SMC identified above.

First, we measured circulating complement levels in 1,003 elderly individuals enrolled in the Prospective Investigation of the Vasculature in Uppsala Seniors (PIVUS) study (*SI Appendix*, Fig. S3*A*) (17). Consistent with prior reports (18), we found that age- and sex-adjusted C3 levels were associated with endothelial-dependent vasodilation (a marker of vascular function), carotid intimal–medial thickness (CIMT; a measure of atherosclerotic plaque burden), and major adverse cardiovascular event rate (MACE; a composite end point which includes incident heart attack and stroke) (Fig. 2*A*). These associations were attenuated after adjusting for inflammatory comorbidities, such as body mass index, indicating they could be confounded by traditional cardiovascular risk factors or alternatively could be on the causal pathway from C3 to atherosclerosis (*SI Appendix*, Fig. S3*B*).

Next, we histologically analyzed postmortem carotid artery specimens. These assays confirmed that C3 expression localizes to the border zone of the necrotic core in human plaques (Fig. 2*B*). To define the source of this C3, we used a permanent epigenetic tag (Myh11-H3K4me2) that persists on SMCs even after phenotypic switching [a method which approximates "human lineage tracing" (19)]. These studies indicated that a subset of dedifferentiated SMCs (i.e., H3K4me2-PLA$^+$/SMA$^-$) express C3 within the lesions of patients with atherosclerotic disease (multiplexed images are shown in Fig. 2*C*, and serial sections are shown in *SI Appendix*, Fig. S3*C*).

Finally, we used an integrative genomics approach to determine if cells with an expression profile similar to the clonal murine SMC also exist in humans. To do this, we intersected the list of homologous human genes derived from the murine Sca1$^+$ SMC gene cluster with tissue-specific RNA-seq data from the 672 individuals included in the Stockholm-Tartu Atherosclerosis Reverse Network Engineering Task (STARNET) biorepository (20). Gene set enrichment analyses confirmed that the Sca1$^+$ SMC signature is in fact present in humans. We found that it is enriched in a subset of the 224 previously described STARNET coexpression modules (Fig. 2*D*), including several that were differentially expressed in subjects with relevant cardiometabolic conditions (*SI Appendix*, Fig. S3*D*). In particular, module 106 (highlighted in gray in Fig. 2*D*) was found to be 1) enriched solely in diseased vascular tissue; 2) associated with CAD by both clinical history and quantitative invasive angiography; and 3) driven by a collection of overlapping inflammatory genes including the key driver, complement C3, and the blood vessel and hematopoietic stem cell marker CD34 (the human Sca1 homolog has not been identified; Fig. 2*E* and *SI Appendix*, Fig. S3 *E–H*).

Taken together, these translational findings confirm that the complement cascade is up-regulated in patients with CAD and indicate that dedifferentiated SMCs may be a source of C3 in the human plaque. Because a cell resembling the murine Sca1$^+$ SMC seems to be present in and relevant to human atherosclerosis, we elected to further pursue its biology in mouse models (21).

C3 Produced by the Sca1$^+$ SMC Induces Proatherogenic Effects Including Paracrine Macrophage Inflammation and Autocrine SMC Proliferation. After establishing its potential clinical relevance, we next set out to map the mechanism by which the clonally expanding murine SMC might promote disease. To do this, we dissociated and cultured Sca1$^+$ and Sca1$^-$ SMCs from lineage-tagged atherosclerotic plaques. Consistent with our RNA-seq data (Fig. 1 *D* and *E*), we found that the conditioned media of Sca1$^+$ SMCs contained high levels of C3 protein (Fig. 3*A*). Application of this secretome to cocultured inflammatory cells induced a variety of proatherogenic effects, including a significant increase in macrophage chemokinesis (Fig. 3*B* and *SI Appendix*,

Downloaded at Palestinian Territory, occupied on December 4, 2021

www.manaraa.com

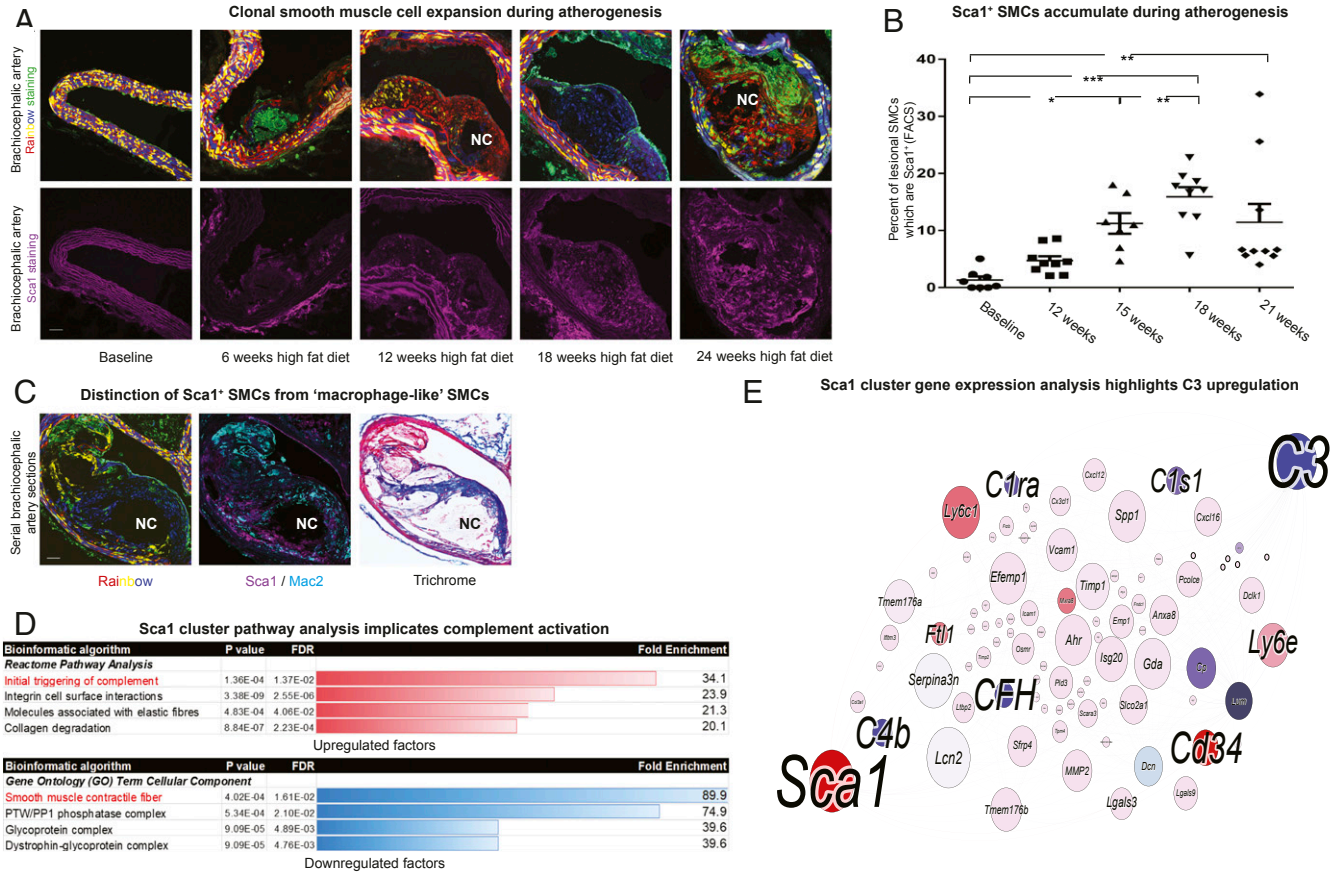

Fig. 1. Atherosclerosis is associated with the clonal expansion of dedifferentiated smooth muscle cells which express complement C3. (*A*) Representative confocal images from multicolor Rainbow lineage-tracing mice exposed to a high-fat Western diet to induce atherogenesis ($n \geq 7$ mice per time point). This model constitutively labels all nonsmooth muscle cells with green fluorescent protein (GFP) and randomly labels all SMC-derived cells (and their progeny) red, blue, or yellow to demonstrate clonal expansion, as shown (*Top*) (see details in *SI Appendix*, Fig. S1*A*). Serial sections are stained for the putative stem cell marker, stem cell antigen-1 (Sca1), as shown (*Bottom*). (*B*) Quantitative fluorescence-activated cell-sorting analyses demonstrate changes in Sca1-expressing SMCs in the aortic arch (including cells from the plaque and the underlying media) during atherogenesis ($n = 9$ per time point). (*C*) Serial sections demonstrate the physical proximity of the dominant SMC clone to the inflammatory necrotic core (NC), and the distinction between Sca1$^+$ SMCs and SMCs which express "macrophage-specific" markers such as Mac2 (see additional examples in *SI Appendix*, Fig. S1*G*). (*D*) Pathway analyses of single-cell RNA-seq data from Sca1$^+$ SMCs isolated from lesions of single-color Tomato lineage-tracing mice demonstrate that the Sca1$^+$ SMC is highly dedifferentiated, down-regulates its contractile machinery, and up-regulates factors related to innate immunity and the classical complement cascade. (*E*) Among the individual genes which are differentially regulated in the Sca1$^+$ SMC cluster, complement C3 is up-regulated 4.4-fold (node size is proportional to fold change; complement factors are highlighted in blue, and factors related to stem cell biology are highlighted in red). Comparisons are made by one-way ANOVA with Tukey's post hoc analysis. $***P < 0.001$, $**P < 0.01$, $*P < 0.05$. Error bars represent the SEM. (Scale bars, 50 μm.)

Fig. S4 *A–E*). C3 immunoprecipitation/depletion reversed these defects, suggesting a causal link. Confirmatory assays with recombinant peptide indicated that C3 also exacerbated the skewing, chemotaxis, and apoptosis of cultured macrophages (*SI Appendix*, Fig. S4 *F–I*). These results suggest that complement elaborated by the Sca1$^+$ SMC may potentiate vascular inflammation, and possibly do so in a paracrine fashion (*SI Appendix*, Fig. S4*J*).

Complement C3 has also previously been shown to trigger SMC proliferation (22). Accordingly, we hypothesized that C3 produced by the Sca1$^+$ SMC might not only stimulate neighboring macrophages but also feed back in an autocrine loop to the clonally expanding SMC itself. Using cell-surface fluorescence-activated cell sorting (FACS) analyses, we found high levels of C3 adsorbed directly on the surface of freshly isolated Sca1$^+$ SMCs (Fig. 3*C*). Consistent with its known mitogenic properties (22), we found that recombinant C3 could trigger cell division and migration in cultured human coronary artery SMCs, and that primary C3^{hi} Sca1$^+$ SMCs had a significant proliferative advantage compared with C3^{lo} Sca1$^-$ SMCs (Fig. 3*D* and *SI Appendix*, Fig. S5 *A–E*).

These data suggest that C3 generated by the Sca1$^+$ SMC might not only trigger the paracrine macrophage inflammation described above but also trigger SMC proliferation in an autocrine fashion. This observation may help explain why the proinflammatory SMCs within the clone expand so quickly, and how they contribute to the physical growth of the atherosclerotic plaque.

C3 Expressed on the Surface of Sca1$^+$ SMCs Also Identifies Those Cells for Phagocytic Removal. As it is degraded, C3 is cleaved into C3a and C3b (*SI Appendix*, Fig. S5*F*) (23). C3a is a potent anaphylatoxin, and is likely responsible for many of the maladaptive changes described above. C3b, on the other hand, is a powerful opsonin signal that triggers programmed cell removal (PrCR), or "efferocytosis" of pathogenic cells (24). C3b has long been recognized as a marker of "nonself" used to flag invading bacteria. More recently, it has also been identified as a "danger signal" applied to the surface of diseased or unwanted tissue (25). In the field of oncology, tumoricidal macrophages have been shown to use related immune-surveillance mechanisms to identify and eradicate precancerous clones before they undergo malignant

Downloaded at Palestinian Territory, occupied on December 4, 2021
www.manaraa.com

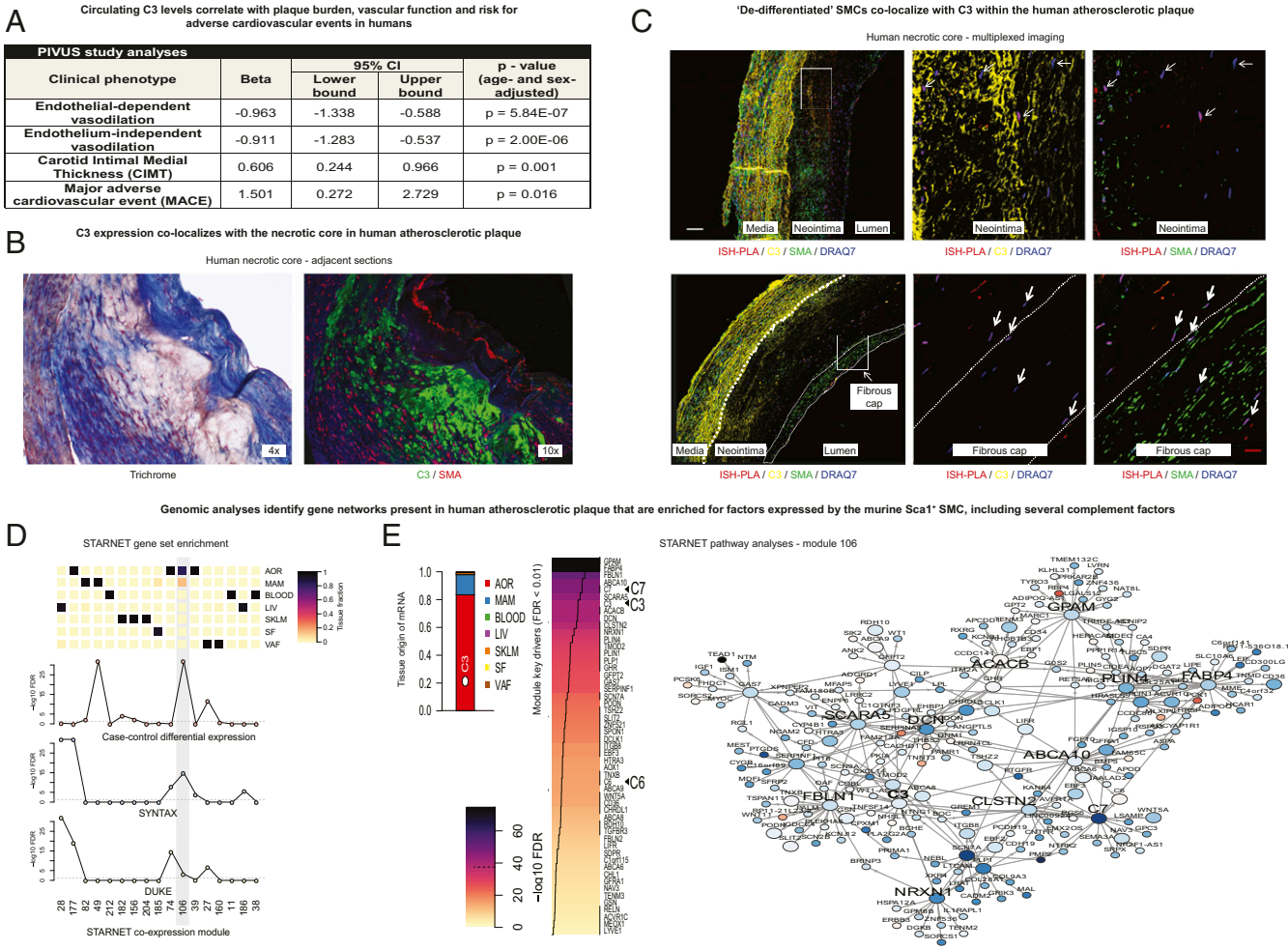

Fig. 2. C3 is associated with risk for clinical cardiovascular disease and is expressed on dedifferentiated SMCs in human atherosclerotic plaque. (*A*) Using data from $n = 1{,}003$ individuals from the PIVUS study, circulating C3 levels were found to be associated with increased carotid intimal–medial thickness, impaired endothelial function, and increased major adverse cardiovascular events in age- and sex-adjusted models. (*B*) Serial sections obtained from the plaques of human subjects undergoing carotid endarterectomy were stained for C3 expression (green) to identify proximity to the necrotic core (trichrome) and differentiated α-SMA–expressing SMCs (red; $n = 6$ samples). (*C*) A permanent proximity ligation assay-based epigenetic probe that "lineage tags" cells which previously expressed MYH11 was used to identify human cells of putative SMC origin (red). Human carotid plaque samples are used to show C3 staining (yellow) on cells which do not express α-SMA (green) but are presumably of SMC origin (red) in the neointima (*Top*). Fibrotic cap samples are used to show the lack of C3 staining on differentiated SMCs (indicated by simultaneous α-SMA and in situ hybridization-proximity ligation assay [ISH-PLA] signal) (*Bottom*). (*D*) By intersecting the list of murine Sca1$^+$ SMC-associated genes (Fig. 1*E*) with multitissue RNA-seq data obtained from $n = 672$ individuals in the STARNET study, we observed enrichment of genes associated with the Sca1$^+$ SMC in a distinct subset of human coexpression modules. Several identified modules were specific to vascular tissue and subjects with angiographically confirmed coronary artery disease. (*E*) The highlighted module (106) was solely expressed in atherosclerotic aorta (AOR) and mammary artery tissue (MAM) (as opposed to nonvascular tissues: blood [BLOOD], liver [LIV], skeletal muscle [SKLM], visceral abdominal fat [VAF], and subcutaneous fat [SF]), differentially expressed in subjects with CAD compared with controls, and correlated with quantitative measures of plaque burden such as Duke and SYNTAX score. Bayesian network modeling indicates that module 106 is driven by several complement factors, including the hub driver gene C3 expressed in AOR tissue. (Scale bars, 50 μm [white] and 10 μm [red].)

transformation (16). Because they are so extensively opsonized (Fig. 3*C*), we hypothesized that the Sca1$^+$ SMC might elicit similar phagocytic clearance mechanisms in lesional macrophages, and that these might constrain expansion of the dominant clone.

In keeping with this hypothesis, primary Sca1$^+$ SMCs freshly isolated from atherosclerotic plaques were found to be highly susceptible to PrCR by professional phagocytes (Fig. 3*E*). Compared with nonopsonized Sca1$^-$ SMCs isolated from the same lesions, they were ~50% more likely to be targeted for clearance. Consistent with these results, the application of complement-rich atherosclerotic serum was found to be sufficient to trigger the engulfment of inflamed and lipid-loaded vascular SMCs in vitro. Heat inactivation of the serum (which neutralizes complement activity) completely inhibited this prophagocytic effect, indicating a causal relationship (*SI Appendix*, Fig. S5 *G–J*).

Taken together, these results suggest that C3 elaborated by the Sca1$^+$ SMC may confer the cell with its proatherogenic properties (via the generation of C3a anaphylatoxins) but also simultaneously flag it as pathologic and in need of phagocytic removal (due to the deposition of C3b opsonins) (23). Thus, the body's conserved immune-surveillance machinery does appear to appropriately detect and respond to the threat presented by the hyperproliferative Sca1$^+$ SMC, at least initially.

Polarized Macrophages Lose the Ability to Sense and Clear C3-Opsonized Targets Such as the Sca1$^+$ SMC. We next set out to determine why these safeguards ultimately fail to prevent clonal expansion in vivo. During atherogenesis, macrophages polarize toward an inflammatory (M1) state (26). We hypothesized that these cells might acquire a defect in immune surveillance, and lose the ability to remove opsonized

Downloaded at Palestinian Territory, occupied on December 4, 2021
www.manaraa.com

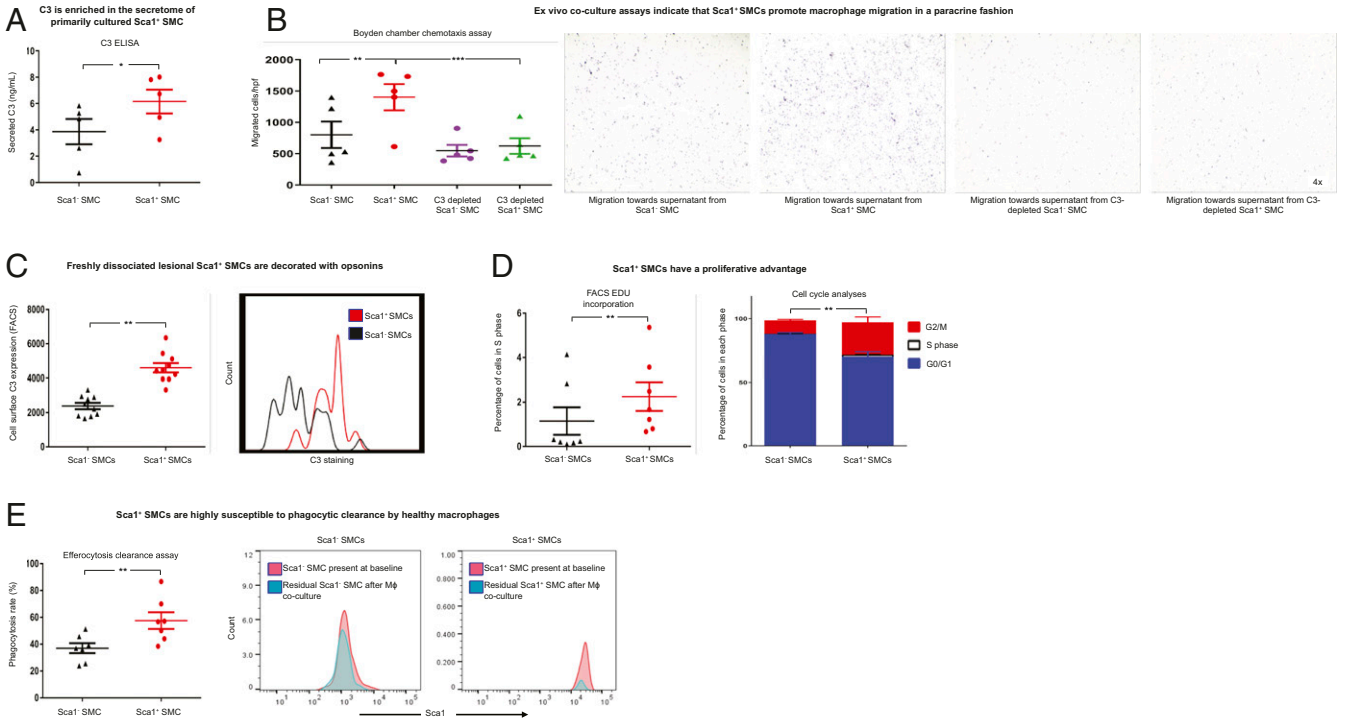

Fig. 3. C3 produced by lesional SMCs induces both pro- and antiatherosclerotic changes in neighboring cells. (*A*) ELISA analyses demonstrate C3 levels in the secretome of Sca1$^+$ and Sca1$^-$ SMCs primarily cultured from atherosclerotic plaques of Tomato mice ($n = 5$ per condition). (*B*) Boyden chamber assays using murine RAW 264.7 macrophages (nuclei stained blue) demonstrate migration rates toward chemotactic factors in the conditioned medium secreted by primary Sca1$^+$ and Sca1$^-$ murine SMCs before (*Left*) and after (*Right*) C3 immunoprecipitation/depletion ($n = 5$ per condition, hpf: high power field). (*C*) FACS histograms demonstrate C3/C3b/iC3b opsonin signals on lesional murine Sca1$^+$ and Sca1$^-$ SMCs quantified by the geometric mean of cell-surface fluorescence intensity ($n = 10$ per condition). (*D*) FACS-based Edu-incorporation assays demonstrate the proliferation rates of Sca1$^+$ and Sca1$^-$ SMCs primarily isolated from atherosclerotic lesions of Tomato mice fed an HFD for 18 wk. (*D*, *Left*) Percentage of cells entering the S phase of mitosis. (*D*, *Right*) Cell-cycle analyses of cells in the S and G2/M phases ($n = 7$ per condition). (*E*) FACS-based efferocytosis assays demonstrate the susceptibility of freshly isolated Sca1$^+$ and Sca1$^-$ SMCs to phagocytic clearance by healthy murine M0 RAW 264.7 macrophages (*Left*; $n = 7$). Representative histograms (*Right*) show the relative numbers of diseased (Annexin$^+$/Tomato$^+$) Sca1$^-$ (*Left*) and Sca1$^+$ (*Right*) SMCs before (red) and after (blue) presentation to healthy RAW 264.7 phagocytes. Comparisons are made by two-tailed paired *t* tests in *A*, *D*, and *E*, Wilcoxon signed-rank test in *C*, and one-way ANOVA with Tukey's post hoc analysis in *B*. $^{***}P < 0.001$, $^{**}P < 0.01$, $^{*}P < 0.05$. Error bars represent the SEM.

SMCs. Accordingly, we repeated the preceding efferocytosis assays under conditions designed to mimic the inflammatory milieu of the atherosclerotic plaque. To do this, we used phagocytes that had been polarized with interferon gamma (IFN-γ).

Interestingly, nonopsonized Sca1$^-$ SMCs were cleared at equivalent (but relatively modest) rates whether they were presented to healthy (M0) or polarized (M1) macrophages (37 vs. 41% efferocytosis rates, respectively; Fig. 4*A*). In contrast, Sca1$^+$ SMCs were rapidly removed only when cocultured with healthy phagocytes, and were largely ignored when presented to M1 macrophages (58 vs. 20% efferocytosis rates, respectively; Fig. 4*B*).

Because of these differences, we hypothesized that lesional phagocytes might lose the capacity to detect targets decorated with "eat me" signals. Consistent with this concept, mechanistic studies using fluorescently labeled complement fragments confirmed that polarized macrophages could not successfully engage opsonin signals. After M1 skewing, macrophages had reduced capacity to bind recombinant iC3b (Fig. 4*C*), and engulfed fewer complement-opsonized latex beads (Fig. 4*D* and *SI Appendix*, Fig. S5 *K–M*).

These studies suggest that the clonal SMC is not intrinsically "inedible." Rather, the C3^{hi} Sca1$^+$ SMC may escape immune surveillance because the phagocytes that reside within the atherosclerotic plaque happen to have a generalized defect in opsonin sensing. Because the Sca1$^+$ SMC may also have an intrinsic growth advantage (Fig. 3*D*), this additional survival advantage may explain how clonal SMCs expand in vivo.

The Noncanonical Up-Regulation of Efferocytosis Molecules on Polarized Macrophages Coincides with Their Loss of Phagocytic Capacity. To investigate why M1 macrophages have reduced capacity to detect cell-surface C3, we measured the expression of the classical opsonin receptor CR3 [also known as Mac1 or CD11b/CD18 (27)] before and after phagocyte polarization. Contrary to our prediction, CD11b levels were not reduced during macrophage skewing (*SI Appendix*, Fig. S6*A*). We therefore hypothesized that M1 macrophages might acquire some other defect that reduces their opsonin-sensing capacity during atherogenesis.

Previously, we showed that inflammatory pathways common to cancer and cardiovascular disease lead to an up-regulation of the key "don't eat me" molecule, CD47 (28–30). Pathological increases of this antiefferocytic signal on the surface of target cells reduce their "edibility" and prevent their homeostatic clearance (31). More recently, however, CD47 has also been shown to signal in *cis* to its receptor, Sirp-α (32), suggesting it could play a role in the immune-surveillance capacity of the lesional phagocyte.

To test whether CD47 might also have an unappreciated role in the lesional phagocyte (beyond its usual role in target cells in the plaque), we measured its expression during macrophage skewing. These experiments showed that CD47 is expressed at a low level on healthy macrophages but is significantly up-regulated on M1 macrophages, especially in the presence of exogenous C3 (*SI Appendix*, Fig. S6 *B–D*). These data raise the interesting possibility that CD47 might be more than a "don't eat me" molecule used by cells to evade phagocytosis. Instead, CD47

Downloaded at Palestinian Territory, occupied on December 4, 2021
www.manaraa.com

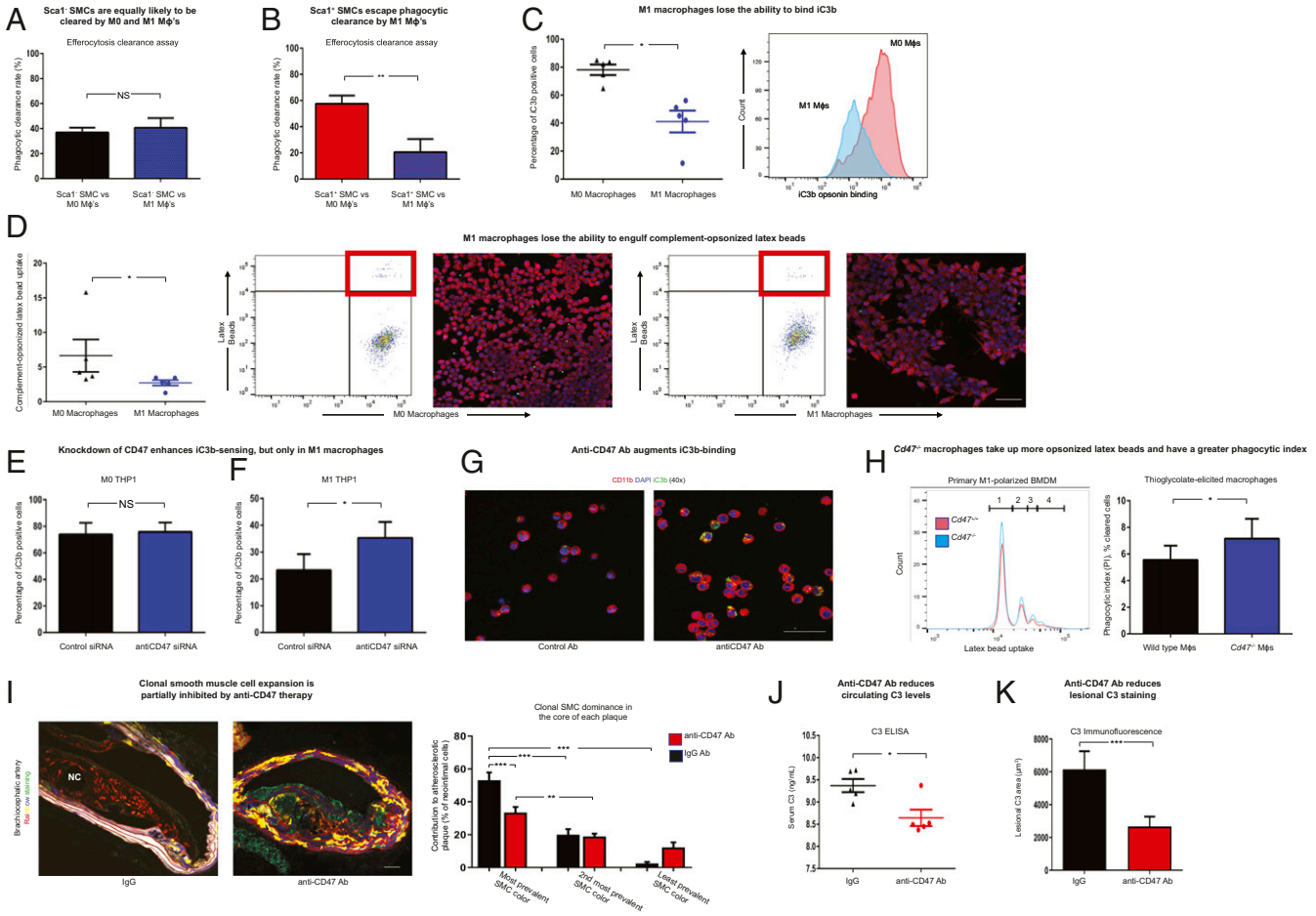

Fig. 4. Blockade of CD47 normalizes the ability of polarized macrophages to recognize complement-opsonized targets, suppresses clonal expansion, and prevents atherosclerosis. (*A*) FACS analyses demonstrate that apoptotic murine Sca1$^-$ SMCs freshly isolated from atherosclerotic lesions were cleared at equivalent rates by healthy M0 and inflammatory M1 murine RAW 264.7 macrophages ($n = 7$ per condition). (*B*) In contrast, FACS analyses demonstrated that the clearance rate of apoptotic Sca1$^+$ SMCs by M1 macrophages was significantly lower than that by healthy M0 RAW 264.7, despite being opsonized ($n = 7$ per condition). (*C*) Compared with basal conditions, M1-polarized THP-1 macrophages were found to have reduced ability to bind iC3b, the opsonin that marks apoptotic cells for complement-dependent efferocytosis ($n = 5$ per condition). Representative histograms indicate a left shift of fluorescently labeled iC3b on M1 (blue) compared with M0 (red) THP-1 macrophages. (*D*) FACS engulfment assays demonstrate the capacity of M0 and polarized M1 human THP-1 macrophages to take up complement-opsonized latex beads ($n = 5$ per condition; representative FACS panels; *Left*). Confirmatory confocal microscopy images (*Right*) of RAW 264.7 macrophages (red) reveal that M1 macrophages bind fewer complement-opsonized latex beads (green) after 30 min of coculture. (*E*) FACS assays demonstrate equivalent binding of fluorescently labeled iC3b to human M0 THP-1 cells before and after CD47 knockdown ($P = 0.56$; $n = 4$ per condition). (*F*) Conversely, knockdown of CD47 increases the capacity of CD47^{hi} human M1 THP-1 cells to bind iC3b ($n = 4$ per condition). (*G*) Representative confocal microscopy images demonstrate that inhibitory anti-CD47 antibodies augment iC3b (green) binding to cell-surface CD11b (red) on human M1 THP-1 cells, relative to cells treated with IgG control Ab ($n = 3$ per condition). (*H*) Representative histograms (*Left*) indicate that M1-polarized bone marrow-derived macrophages (BMDMs) isolated from CD47 knockout mice (blue) take up more complement-opsonized latex beads than cells isolated from WT mice (red; the number of latex bead[s] taken up is indicated on the *x* axis, and the number of phagocytes is indicated on the *y* axis). Similarly, FACS-based engulfment assays demonstrate that thioglycolate-elicited peritoneal macrophages from CD47 knockout mice have a higher phagocytic index than cells isolated from age-matched WT mice ($n = 5$ per condition; *Right*). (*I*) In contrast to lesions from Rainbow mice treated with control IgG Ab which are almost universally populated by a single SMC clone (see example of a red clone near the necrotic core; *Left*), lesions from Rainbow mice treated with anti-CD47 Ab demonstrate a stochastic assortment of SMCs within the neointima under the fibrotic cap (see the example with a random collection of colors; *Right*). Blinded quantitative analysis of plaques confirms that anti-CD47 Ab treatment is associated with an overall reduction in neointimal SMC content as well as clonal dominance in the core of BCA (brachiocephalic artery) lesions ($n = 9$ mice per condition; *Right*). Additional phenotyping and quantification of plaque stability indices, including an absence of change in SMC content in the fibrous cap, are provided in *SI Appendix*, Figs. S7 and S8. (*J* and *K*) Anti-CD47 Ab-treated mice have reduced C3 levels in their circulation (*J*) ($n = 5$ per condition; ELISA) and within their BCA lesions (*K*) ($n = 9$ animals per group; immunofluorescence staining). Comparisons were made by two-tailed *t* tests in *A*–*C*, *E*, *F*, *H*, *J*, and *K*, Mann–Whitney *U* test in *D*, and one-way ANOVA with Tukey's post hoc analysis in *I*. ***$P < 0.001$, **$P < 0.01$, *$P < 0.05$. NS, not significant. Error bars represent the SEM. (Scale bars, 50 μm.)

could also have an undescribed role in the direct regulation of inflamed macrophage "appetite" and its propensity to sense "eat me" signals, such as complement C3b.

CD47 Can Be Translationally Targeted to Restore Immune Surveillance and Suppress Clonal SMC Expansion in the Atherosclerotic Plaque. We next sought to prove whether CD47 has a causal role in opsonin sensing. To do this, we tested whether knockdown or knockout of CD47 could restore the ability of polarized macrophages to clear targets decorated with complement.

As predicted based on their low basal CD47 expression, M0 macrophage physiology was not altered by treatment with an anti-CD47 small interfering RNA (siRNA) (Fig. 4*E*). Similar findings were observed in primarily cultured cells. For example,

Downloaded at Palestinian Territory, occupied on December 4, 2021
www.manaraa.com

freshly isolated CD47 knockout and wild-type macrophages had essentially identical baseline phagocytic capacities (*SI Appendix*, Fig. S7*A*). On the other hand, knockdown of CD47 in immortalized M1 macrophages led to a significant increase in their ability to sense and bind C3b (Fig. 4 *F* and *G*). In keeping with this observation, polarized CD47 knockout macrophages were found to more avidly take up opsonized latex beads and complement-decorated target cells than wild-type macrophages (Fig. 4*H* and *SI Appendix*, Fig. S7 *B* and *C*). These findings indicate that CD47 not only suppresses target cell edibility but also reduces the capacity of atherogenic M1 macrophages to identify and remove opsonized targets, such as the $Sca1^+$ SMC.

Given these findings, we hypothesized that blockade of CD47 might restore macrophage function, augment elimination of C3-expressing SMCs, and suppress clonal expansion in vivo. We reasoned that such an approach could have translational relevance, given our prior reports showing that CD47 signaling is pathologically up-regulated during both mouse and human atherogenesis (29, 33). To test whether inhibition of CD47 could restore immune surveillance, we treated Rainbow mice with anti-CD47 antibody (Ab). Compared with a control immunoglobulin G (IgG) Ab, anti-CD47 Ab treatment was associated with a reduction in clonal expansion and a lower likelihood that a plaque was dominated by a single SMC clone (Fig. 4*I* and *SI Appendix*, Fig. S7 *D–F*). More individually resolvable SMC patches were observed after treatment, indicating a shift from an oligo- to polyclonal status (*SI Appendix*, Fig. S7*G*). We found that these benefits did not occur as the result of indiscriminate suppression of all lesional SMCs, as there was no impact on the number of nonopsonized SMCs in the fibrous cap (*SI Appendix*, Fig. S8 *A* and *B*). Moreover, these effects occurred independent of the anti-CD47 Ab's described role in the removal of necrotic debris, and were not associated with a reduction in lesional macrophage content, arguing for a specific mechanism of action (*SI Appendix*, Fig. S8 *A* and *B*). Importantly, we did not observe an increase in any feature of plaque vulnerability (e.g., fibrous cap destabilization, intraplaque hemorrhage), as could be a theoretical concern with nontargeted inhibition of all SMC investment in the plaque. We also found that elimination of the dominant clone was associated with a reduction in both lesional and circulating C3 levels (Fig. 4 *J* and *K* and *SI Appendix*, Fig. S8*C*), suggesting a potential reduction in vascular inflammation. While future studies with cell-specific knockouts will be helpful to confirm the mechanism of benefit, these data suggest that clonal expansion is not an irreversible process and that the phenomenon might be susceptible to precision targeting in vivo.

Discussion

Taken together, these data provide fundamental insights into the decades-old observation that atherosclerosis has a clonal origin (14), and indicate that the process may represent a translational target. Specifically, we find that (at least a subset of) dedifferentiated SMCs pathologically activate the anaphylatoxin arm of the complement cascade, providing a possible mechanism by which they might trigger vascular inflammation. Integrated genomic studies suggest similar pathways may be active in human atherosclerosis. We report that these cells develop a survival advantage not only because they are hyperproliferative but also because they escape immune surveillance, despite being extensively opsonized. To explain this defect, we describe a role for efferocytosis molecule redistribution during macrophage skewing, highlighting that "don't eat me" molecules may inhibit phagocyte appetite as strongly as they suppress target cell edibility in the plaque. We show that the M1 macrophage's inability to detect complement can be overcome, and that blockade of CD47 is sufficient to normalize opsonin sensing, reactivate the targeted removal of $Sca1^+$ SMCs, and partially suppress clonality in vivo. Notably, we observed that these benefits are not indiscriminate, and that such an approach is not confounded by the simultaneous depletion of plaque-stabilizing SMCs in the fibrous cap.

Future studies are necessary to fully define the origins of the $Sca1^+$ SMC and its interaction with other cells in the atherosclerotic plaque. Recent studies suggest there may be a pool of specialized medial progenitor cells that are "primed" for expansion (11). However, it remains unclear 1) what upstream genetic/epigenetic mechanisms permit or promote SMC clonality; 2) whether all clonal cells transiently pass through a $Sca1^+$ state; and 3) if these cells may actively suppress other lesional SMCs. Furthermore, clonal hematopoiesis has now been definitively associated with risk for cardiovascular disease in humans (34). Because cross-talk between the myeloid compartment and vascular SMCs is now recognized as a determinant of clonality in mice (8), the interplay between these lineages merits further investigation. Such efforts are particularly important given that recent clinical trials have validated the "inflammatory hypothesis" of atherosclerosis but also highlighted the risks associated with nontargeted antiinflammatory therapies, including increased susceptibility to fatal infection (35). A key area for exploration will be to identify how SMC fate is determined, and if "therapeutic biasing" approaches can be used to precision target SMC progeny away from potentially deleterious phenotypes, particularly for those pathways that have been causally related to CAD via human genetics studies (7, 12, 36, 37).

From a translational perspective, it is important to note that humanized anti-CD47 therapies have recently shown promise in early-phase oncology studies (38, 39). These proefferocytic and pro-PrCR drugs reactivate macrophage phagocytosis, and are thought to reduce tumor burden by preventing unchecked expansion of cancer cells and cancer stem cells. Given the increasingly recognized commonalities between cancer and cardiovascular disease (15), it is interesting to consider the possibility that these therapies could be adapted to target Benditt's atherosclerotic progenitor cell as well. Such an approach might suppress the clonal component of atherosclerosis and reduce cardiovascular risk in a manner not possible with currently available lipid-lowering and antihypertensive therapies.

Materials and Methods

Study Design. The prespecified objective of this study was to characterize clonal SMC expansion during atherosclerosis. This was performed using a combination of indelible murine lineage-tracing models. Mechanistic studies, including those based on single-cell RNA sequencing and ex vivo physiology assays, were performed with primary cells freshly isolated from dissociated plaques. Confirmatory assays were performed with immortalized mouse and human cell lines. Translational studies included those using an assortment of human tissues from previously published biobanks, as well as a randomized therapeutic intervention study with an investigational antibody thought to have antiatherosclerotic properties. All experiments included at least three replicates, with the actual "*n*" specified in each figure legend. Detailed methods are provided within *SI Appendix*, and are briefly summarized below.

Research Subjects.

Mouse models. Two SMC lineage-tracing models were developed for this study, as detailed in *SI Appendix*, Figs. S1 and S2. These include a multicolor Rainbow reporter (Myh11-Cre^{ERT2}, $Rosa26^{Rainbow/+}$, $ApoE^{-/-}$ mice) and a single-color Tomato reporter (Myh11-Cre^{ERT2}, $Rosa26^{tdTomato/tdTomato}$, $ApoE^{-/-}$ mice). After treatment with tamoxifen, mice were fed a high-fat Western diet (HFD) containing 21% anhydrous milk fat, 19% casein, and 0.25% cholesterol for different periods of time as indicated in each experiment to induce atherosclerosis. Clonality was quantified in a blinded manner using Volocity software analyses of postmortem brachiocephalic artery sections, as described in *SI Appendix, Methods* and shown in *SI Appendix*, Fig. S7. All animal studies were approved by the Stanford University Administrative Panel on Laboratory Animal Care (Protocol 27279).

Human samples. Human samples utilized in this report were obtained from the PIVUS study (n = 1,016 subjects) (17), STARNET study (n = 672 subjects) (20), or Munich Vascular Biobank (n = 6 subjects) (40). The PIVUS study was

Downloaded at Palestinian Territory, occupied on December 4, 2021

www.manaraa.com

approved by the Ethics Committee of the University of Uppsala and all participants gave informed consent. Subjects from the STARNET study provided informed consent (Ethical Approvals Dnr 154/7 and 188/M-12 from Tartu University Hospital). Biospecimens in the Munich Vascular Biobank were approved by the local hospital ethics committee (2799/10, Ethikkommission der Fakultät für Medizin der Technischen Universität München). Informed consent was obtained from all patients. Vascular function testing, coronary angiography, carotid artery duplex imaging, histology, bioinformatics, and outcome analyses were performed as described in *SI Appendix, Methods* and associated references.

Single-Cell RNA Sequencing and Pathway Analysis. Lineage-tagged (Tdt^+) SMC-derived cells freshly dissociated from the aortic arches of atherosclerotic Tomato mice fed 18 wk of an HFD were subjected to single-cell RNA sequencing using C1 96-well Open App IFC plates (100-8135; Fluidigm) in collaboration with the Stanford Genome Sequencing Service Center on an Illumina HiSeq 4000 instrument. Differential gene expression was quantified with SCDE, and pathway analyses were performed via GO and DAVID, using P value < 0.01 and false discovery rate (FDR) < 0.05. Datasets are available at https://www.ncbi.nlm.nih.gov/bioproject/626450.

In Vitro Assays. Cells used in this report included primary cells and immortalized cell lines from both mice and humans. Their isolation and culture conditions are described in detail in *SI Appendix, Methods*. Briefly, primary $Sca1^+$ and $Sca1^-$ SMCs were expanded from the digested and FACS-sorted lineage-traced plaques described above. Primary bone marrow-derived and peritoneal macrophages were isolated from wild-type (WT) and $CD47^{-/-}$ mice on a C57BL/6 mouse background. Commercially available macrophage cell lines included murine RAW 264.7 cells (TIB71; ATCC) grown in Dulbecco's modified Eagle's medium-growth media and human THP-1 cells (TIB-202; ATCC) grown in RPMI-1640 media, each containing 10% fetal bovine serum (FBS). Human coronary artery SMCs (CC-2583; Lonza; passages 3 to 6) propagated in SMC basal medium supplemented with an SmGM-2 SingleQuots Kit and 10% FBS were also used.

A wide variety of commonly used in vitro physiology assays were performed, including Boyden chamber chemotaxis assays (8-μm pore; Sigma), membrane attack complex formation assays (C5b-9 Ab), cell-scratch assays (using a P200 tip), TUNEL assays (In Situ Death Detection Kit; Sigma), and TaqMan gene expression assays (TRIzol extraction, NanoDrop RNA quantification, and analysis on a ViiA7 Real-Time PCR machine) (29, 36, 41). In addition, a number of FACS assays were performed including both sorting experiments (LSRII-UV), cell-proliferation assays (Edu, 5-ethynyl-2′-deoxyuridine, incorporation), and phagocytosis/efferocytosis assays, as previously described (29). Most assays included stimulation with complement factors or a variety of proatherogenic cytokines. These included recombinant human complement C3 (204885) from Millipore Sigma, and recombinant mouse C3 (P3343) obtained from Novus Biologicals. Cytokines used in this study included mouse IFN-γ (485-MI-100) and human IFN-γ (285-IF-100) from R&D Systems and lipopolysaccharide (L2630) from Sigma. A full list of reagents, including antibodies, FACS parameters, and related experimental details, is provided in *SI Appendix, Methods*.

In Situ Hybridization-Proximity Ligation Assay. In addition to the routine immunofluorescence staining and confocal microscopy described in *SI Appendix*, we also adapted a previously described epigenetic SMC marker that can be used to approximate lineage tracing on human samples (19). Using 5-μm sections from formalin-fixed paraffin-embedded carotid plaques, we performed proximity ligation assays for H3K4dime and biotin-labeled *MYH11* probes which were detected using a rabbit anti-biotin antibody (1:100; ab53494; Abcam) and mouse anti-dimethyl histone H3 (Lys4) (1:100; 05-1338; Millipore Sigma) by the Duolink In Situ Detection Reagents Red Kit (DUO92008-30RXN) or FarRed Kit (DUO92013-30RXN) (Sigma). On some tissue sections, nuclei were stained with Draq7 (564904; BD Pharmingen) to minimize the background of autofluorescence around the necrotic core.

Atherosclerosis Intervention Studies. To evaluate the effect of anti-CD47 antibody therapy on SMC clonality in the atherosclerotic lesion, 8-wk-old Rainbow mice were injected with tamoxifen as described above, and then initiated on an HFD at the age of 9 wk and injected with either 200 μg of the inhibitory anti-CD47 antibody (MIAP410; BioXCell; $n = 9$) or IgG1 control (MOPC-21; BioXCell; $n = 9$) intraperitoneally every other day for 18 wk (29). At 27 wk of age, the mice were killed and the aortic trees were perfused with phosphate-buffered saline. The aortic arch was dissected carefully from any surrounding tissues, fixed with 4% paraformaldehyde, embedded in OCT, and sectioned at 7-μm thickness from the base of the aortic arch to the base of the innominate artery for all subsequent morphometric analyses, which are described in detail in *SI Appendix, Methods*.

Statistical Analysis. Results were analyzed by SPSS Statistics 20 and GraphPad Prism 5 for statistical significance between treatment groups. The normality of data for figures was determined by performing D'Agostino and Pearson omnibus normality tests. The homogeneity of variance was determined by performing either an F test or a Levene's test. Normally distributed data of equal variance were analyzed using parametric tests, including two-tailed Student t tests, one-way ANOVA with Tukey's, or Dunnett's post hoc comparisons as indicated in the figure legends. Data that did not meet either assumption were analyzed using nonparametric tests, including the Mann–Whitney U test, Wilcoxon signed-rank test, Kruskal–Wallis test, or Friedman test as indicated in the figure legends. Data are presented as mean ± SEM. P values < 0.05 were considered significant.

Data Availability. The datasets generated in this study are available at https://www.ncbi.nlm.nih.gov/bioproject/626450.

ACKNOWLEDGMENTS. This study was supported by the NIH (R35 HL144475, R01 HL125224, and R01 HL123370 to N.J.L.; R01 HL125863 to J.L.M.B.), American Heart Association (19EIA34770065 to N.J.L.; 18POST34030084 to Y.W.; A14SFRN20840000 to J.L.M.B.), Swedish Research Council and Heart Lung Foundation (2018-02529 and 20170265 to J.L.M.B.), Deutsche Forschungsgemeinschaft (JA 2869/1-1:1 to K.-U.J.), and Fondation Leducq ("PlaqOmics" 18CVD02 to N.J.L., J.L.M.B., C.L.M., G.P., and G.K.O.). We acknowledge Stefan Gustafsson, Tom Quertermous, Robert Wirka, and Milos Pjanic for critical input on the manuscript, Zhichao Ni (Qingbo Xu lab, King's College) for advice on $Sca1^+$ SMC culture, and the Stanford Shared FACS Facility (via NIH S10 Shared Instrument Grant S10RR027431-01) and Cell Sciences Imaging Facility for access to core facilities.

1. World Health Organization, The top 10 causes of death (2018). https://www.who.int/en/news-room/fact-sheets/detail/the-top-10-causes-of-death. Accessed 20 January 2020.
2. P. Libby, P. M. Ridker, G. K. Hansson, Progress and challenges in translating the biology of atherosclerosis. *Nature* **473**, 317–325 (2011).
3. R. Ross, Atherosclerosis—An inflammatory disease. *N. Engl. J. Med.* **340**, 115–126 (1999).
4. D. Gomez, G. K. Owens, Smooth muscle cell phenotypic switching in atherosclerosis. *Cardiovasc. Res.* **95**, 156–164 (2012).
5. C. S. Robbins *et al*., Local proliferation dominates lesional macrophage accumulation in atherosclerosis. *Nat. Med.* **19**, 1166–1172 (2013).
6. L. S. Shankman *et al*., KLF4-dependent phenotypic modulation of smooth muscle cells has a key role in atherosclerotic plaque pathogenesis. *Nat. Med.* **21**, 628–637 (2015).
7. J. Chappell *et al*., Extensive proliferation of a subset of differentiated, yet plastic, medial vascular smooth muscle cells contributes to neointimal formation in mouse injury and atherosclerosis models. *Circ. Res.* **119**, 1313–1323 (2016).
8. A. Misra *et al*., Integrin beta3 regulates clonality and fate of smooth muscle-derived atherosclerotic plaque cells. *Nat. Commun.* **9**, 2073 (2018).
9. K. Jacobsen *et al*., Diverse cellular architecture of atherosclerotic plaque derives from clonal expansion of a few medial SMCs. *JCI Insight* **2**, 95890 (2017).
10. S. Feil *et al*., Transdifferentiation of vascular smooth muscle cells to macrophage-like cells during atherogenesis. *Circ. Res.* **115**, 662–667 (2014).
11. L. Dobnikar *et al*., Disease-relevant transcriptional signatures identified in individual smooth muscle cells from healthy mouse vessels. *Nat. Commun.* **9**, 4567 (2018).
12. R. C. Wirka *et al*., Atheroprotective roles of smooth muscle cell phenotypic modulation and the TCF21 disease gene as revealed by single-cell analysis. *Nat. Med.* **25**, 1280–1289 (2019).
13. M. W. Majesky *et al*., Differentiated smooth muscle cells generate a subpopulation of resident vascular progenitor cells in the adventitia regulated by Klf4. *Circ. Res.* **120**, 296–311 (2017).
14. E. P. Benditt, J. M. Benditt, Evidence for a monoclonal origin of human atherosclerotic plaques. *Proc. Natl. Acad. Sci. U.S.A.* **70**, 1753–1756 (1973).
15. D. DiRenzo, G. K. Owens, N. J. Leeper, "Attack of the clones": Commonalities between cancer and atherosclerosis. *Circ. Res.* **120**, 624–626 (2017).
16. T. Reya, S. J. Morrison, M. F. Clarke, I. L. Weissman, Stem cells, cancer, and cancer stem cells. *Nature* **414**, 105–111 (2001).
17. L. Lind, N. Fors, J. Hall, K. Marttala, A. Stenborg, A comparison of three different methods to evaluate endothelium-dependent vasodilation in the elderly: The Prospective Investigation of the Vasculature in Uppsala Seniors (PIVUS) study. *Arterioscler. Thromb. Vasc. Biol.* **25**, 2368–2375 (2005).
18. E. Hertle *et al*., Distinct associations of complement C3a and its precursor C3 with atherosclerosis and cardiovascular disease. The CODAM study. *Thromb. Haemost.* **111**, 1102–1111 (2014).

MEDICAL SCIENCES
Downloaded at Palestinian Territory, occupied on December 4, 2021
www.manaraa.com

19. D. Gomez, L. S. Shankman, A. T. Nguyen, G. K. Owens, Detection of histone modifications at specific gene loci in single cells in histological sections. *Nat. Methods* **10**, 171–177 (2013).
20. O. Franzén *et al*., Cardiometabolic risk loci share downstream *cis*- and *trans*-gene regulation across tissues and diseases. *Science* **353**, 827–830 (2016).
21. S. M. Schwartz, R. Virmani, M. W. Majesky, An update on clonality: What smooth muscle cell type makes up the atherosclerotic plaque? *F1000 Res.* **7**, F1000 Faculty Rev-1969 (2018).
22. F. Verdeguer *et al*., Complement regulation in murine and human hypercholesterolemia and role in the control of macrophage and smooth muscle cell proliferation. *Cardiovasc. Res.* **76**, 340–350 (2007).
23. A. Erdei *et al*., The versatile functions of complement C3-derived ligands. *Immunol. Rev.* **274**, 127–140 (2016).
24. M. Martin, A. M. Blom, Complement in removal of the dead—Balancing inflammation. *Immunol. Rev.* **274**, 218–232 (2016).
25. P. F. Zipfel, C. Skerka, Complement regulators and inhibitory proteins. *Nat. Rev. Immunol.* **9**, 729–740 (2009).
26. K. J. Moore, I. Tabas, Macrophages in the pathogenesis of atherosclerosis. *Cell* **145**, 341–355 (2011).
27. M. Kim, C. V. Carman, T. A. Springer, Bidirectional transmembrane signaling by cytoplasmic domain separation in integrins. *Science* **301**, 1720–1725 (2003).
28. P. A. Betancur *et al*., A CD47-associated super-enhancer links pro-inflammatory signalling to CD47 upregulation in breast cancer. *Nat. Commun.* **8**, 14802 (2017).
29. Y. Kojima *et al*., CD47-blocking antibodies restore phagocytosis and prevent atherosclerosis. *Nature* **536**, 86–90 (2016).
30. Y. Kojima, I. L. Weissman, N. J. Leeper, The role of efferocytosis in atherosclerosis. *Circulation* **135**, 476–489 (2017).
31. S. J. Gardai *et al*., Cell-surface calreticulin initiates clearance of viable or apoptotic cells through *trans*-activation of LRP on the phagocyte. *Cell* **123**, 321–334 (2005).
32. B. H. Hayes *et al*., Macrophages show higher levels of engulfment after disruption of *cis* interactions between CD47 and the checkpoint receptor SIRPα. *J. Cell Sci.* **133**, jcs237800 (2020).
33. A. M. Flores *et al*., Pro-efferocytic nanoparticles are specifically taken up by lesional macrophages and prevent atherosclerosis. *Nat. Nanotechnol.* **15**, 154–161 (2020).
34. S. Jaiswal *et al*., Clonal hematopoiesis and risk of atherosclerotic cardiovascular disease. *N. Engl. J. Med.* **377**, 111–121 (2017).
35. P. M. Ridker *et al*.; CANTOS Trial Group, Antiinflammatory therapy with canakinumab for atherosclerotic disease. *N. Engl. J. Med.* **377**, 1119–1131 (2017).
36. Y. Kojima *et al*., Cyclin-dependent kinase inhibitor 2B regulates efferocytosis and atherosclerosis. *J. Clin. Invest.* **124**, 1083–1097 (2014).
37. V. Nanda *et al*., Functional regulatory mechanism of smooth muscle cell-restricted LMOD1 coronary artery disease locus. *PLoS Genet.* **14**, e1007755 (2018).
38. R. Advani *et al*., CD47 blockade by Hu5F9-G4 and rituximab in non-Hodgkin's lymphoma. *N. Engl. J. Med.* **379**, 1711–1721 (2018).
39. B. I. Sikic *et al*., First-in-human, first-in-class phase I trial of the anti-CD47 antibody Hu5F9-G4 in patients with advanced cancers. *J. Clin. Oncol.* **37**, 946–953 (2019).
40. J. Pelisek *et al*., Biobanking: Objectives, requirements, and future challenges—Experiences from the Munich Vascular Biobank. *J. Clin. Med.* **8**, E251 (2019).
41. V. Nanda *et al*., CDKN2B regulates TGFβ signaling and smooth muscle cell investment of hypoxic neovessels. *Circ. Res.* **118**, 230–240 (2016).

Downloaded at Palestinian Territory, occupied on December 4, 2021

www.manaraa.com